NANO LETTERS

2007
Vol. 7, No. 8
2291−2294

A Carbon Nanotube Field Effect Transistor with a Suspended Nanotube Gate

Yury A. Tarakanov* and Jari M. Kinaret

Department of Applied Physics, Chalmers University of Technology, SE-412 96 Gothenburg, Sweden

Received April 16, 2007; Revised Manuscript Received June 4, 2007

ABSTRACT

We investigate theoretically field effect transistors based on single-walled carbon nanotubes (CNTFET) and explore two device geometries with suspended multiwalled carbon nanotubes (MWNT) functioning as gate electrodes. In the two geometries, a doubly or singly clamped MWNT is electrostatically deflected toward the transistor channel, allowing for a variable gate coupling and leading to, for instance, a superior subthreshold slope. We suggest that the proposed designs can be used as nanoelectromechanical switches and as detectors of mechanical motion on the nanoscale.

Carbon nanotubes exhibit a range of properties that make them well suited for nanoelectromechanical devices. They are inherently hollow, light structures with extraordinary stiffness, which opens the route to fast mechanical action. Carbon-nanotube-based nanoelectromechanical devices have been the subject of extensive studies over the last several years, and numerous devices such as nanoscale memory elements[1,2] or switches[3−5] and tunable RF components[6−8] have been discussed theoretically and demonstrated experimentally. In many cases, the agreement between theoretical predictions and experimental observations is remarkably good.[8,9]

The electrical properties of carbon nanotubes cover metallic and semiconducting behaviors and can be used to fabricate electronic circuits of increasing complexity.[10,11] One-dimensional field effect transistors based on single-walled carbon nanotubes have demonstrated excellent electrical characteristics and are competitive with silicon-based solutions.[12]

In this work, we investigate two designs that utilize mechanically deformable metallic nanotubes as suspended gate electrodes for CNTFETs. We show that the mechanical degree of freedom may be used to improve the electrical characteristics of the transistors. In particular, we find that suspended gate CNTFETs have subthreshold slopes that are not limited by the thermal $S = k_B T \ln(10)$ per decade result (60 mV/decade at room tempearature) but may be substantially steeper; this is to be contrasted with stationary CNTFETs that typically exhibit less steep switching ($S \approx$ 100 mV/decade).[12] The general result that mechanical motion can be used to obtain sharper switching is well-known;[13,14] we demonstrate this for realistic nanoscale devices. In the structures that we investigate, the conductance of the CNTFET depends superexponentially on the gate voltage, which causes S to vary as a function of the gate voltage. A static version of one of the structures has recently been implemented experimentally.[15]

The two designs of suspended-gate CNTFETs we consider are schematically shown in Figure 1. Both designs comprise a semiconducting single-walled carbon nanotube (SWNT), attached to source and drain electrodes and lying on a SiO_2 substrate that we take to be 400 nm thick. The two designs differ on how the metallic MWNT suspended gate is mounted: in the first one, we use a doubly clamped nanotube beam (Figure 1A), while in the second one the suspended gate comprises a singly clamped nanotube cantilever (Figure 1B). For the second design, we consider two implementations with different distances between the suspended gate and the CNTFET and different dimensions of the electrode that is used to electrostatically actuate the MWNT. We refer to this electrode as a gate, and the voltage applied to it as the gate voltage (V_{gate}). The MWNT is referred to as the MWNT gate, and corresponding voltage V_{MWNT}. The geometry of the device is such that the SWNT lies below the center of MWNT in design 1 and below the free tip of the MWNT in designs 2a and 2b (Table 1), which leads to the best sensitivity to the deflection of the MWNT. A planar metallic back gate is incorporated beneath the substrate layer. In the mode of operation we consider in this article, voltage on the back gate (V_{BG}) is kept fixed.

* Corresponding author. E-mail: tarakano@chalmers.se. Telephone: +46 31 772 2962. Fax: +46 31 416984.

10.1021/nl070891+ CCC: $37.00
Published on Web 06/30/2007

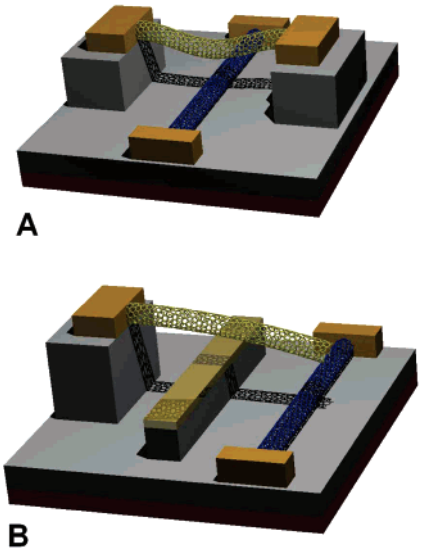

Figure 1. Schematic drawings of the proposed designs. (A) Design 1, (B) designs 2a and 2b. Blue tubes are SWNTs, and yellow tubes are metallic MWNTs.

Table 1. Parameters Used for CNTFET Simulations[a]

parameter	design 1	design 2a	design 2b
SWNT length	1000	1000	1000
SWNT diameter	1.7	1.7	1.7
source and drain height	10	10	10
source and drain width	400	400	400
MWNT length	2000	1000	1000
support height	30	40	60
gate bar height		25	40
D_o	5	30	30
D_i	2	20	20
E (TPa)	1.2	0.4	0.4
source voltage (V)	0	0	0
drain voltage (V)	0.05	0.05	0.05
V_{MWNT} (V)		2	3
V_{BG} (V)	−7/−8	−2	−2

[a] Lengths are given in nm. The gate electrode in designs 2a and 2b is 500 nm long and 100 nm wide and located 400 nm from the MWNT support.

In both designs, a SWNT with source and drain contacts and back gate forms a conventional CNTFET. As a negative voltage is applied to the back gate, holes are injected into the SWNT, forming a conducting channel. At the same time, by applying V_{MWNT}, the suspended MWNT is charged positively so that it electrostatically repels the holes in the SWNT, creating a potential barrier in the middle of the latter and thus reducing the channel conductance of the CNTFET. Thus, the barrier height and width are modulated by both deflection of the MWNT and V_{MWNT}.

In design 1, the channel conductance is lowered by increasing V_{MWNT}. At the same time, electrostatic forces between the MWNT, the polarized silicon dioxide substrate, and the back gate cause the MWNT to bend toward substrate and the CNTFET, which results in a sharper turn-off of the FET conductance.

In contrast, in designs 2a and 2b, the transistor is operated at fixed V_{MWNT}. The potential barrier in the channel is modulated only by the deflection of the MWNT, which is controlled by the voltage applied to the stationary gate electrode. To increase the actuation efficiency, the gate electrode is raised above substrate surface.

Charge transport is known to be diffusive in sufficiently long semiconducting SWNT channels.[16,17] We describe the monopolar charge transport in the SWNT by a continuity equation for holes

$$\frac{\partial_p(x,t)}{\partial t} = -\frac{1}{e}\frac{\partial j_p(x,t)}{\partial x} \tag{1}$$

and the diffusion-drift equation

$$j_p(x,t) = ep(x,t)v_p(F,p) - eD_p(F,p)\frac{\partial_p(x,t)}{\partial x} \tag{2}$$

where p is hole density, j_p is hole current density, F is electric field strength, v_p and D_p are drift velocity and diffusion coefficient for holes, respectively, and e is the elementary charge. The dependence of the drift velocity $v_p(F,p)$ on electric field and concentration has been determined by Perebeinos et al.[18] and Zhou et al.[19] We describe the charge transfer between the metallic drain and source electrodes and the semiconducting SWNT channel using thermionic emission and tunneling.[16]

The electric field strength F in the SWNT is obtained by solving the Poisson equation for the system including metallic bodies (back gate, source, and drain for the SWNT, the MWNT, and the gate), dielectric substrate layer, and the SWNT with a known charge density distribution $\rho(\mathbf{r})$

$$\Delta\phi(\mathbf{r}) = 4\pi\rho(\mathbf{r}) \tag{3}$$

with boundary conditions defined by the geometry of the metallic bodies and voltages applied to them. We solve the eq 3 numerically using a boundary element method.[20,21]

The transverse deflection of CNT can be described as that of an elastic beam[22]

$$-T\frac{\partial^2 u}{\partial x^2} + \frac{\partial^2}{\partial x^2}EI\left(\frac{\partial^2 u}{\partial x^2}\right) = f(x) \tag{4}$$

where $u(x)$ is the vertical deviation of the tube, E is the effective Young modulus of the nanotube, $T = T_0 + (EA/2L)\int_0^L (\mathrm{d}u/\mathrm{d}x)^2\,\mathrm{d}x$ its tension,[8] L its length, $I = \pi(D_o^4 - D_i^4)/64$, and $A = \pi(D_o^2 - D_i^2)/4$ the cross-sectional moment of inertia and cross-sectional area, respectively, T_0 the residual tension, D_o and D_i the outer and inner diameters, respectively, and $f(x)$ is electrostatic force applied to the MWNT. The force $f(x)$ depends on the deflection of the MWNT $u(x)$ because the latter affects the capacitance between the MWNT and other parts of the system, which in turn influences the charge distributions. The mechanical eq 4 is therefore solved self-consistently with the electronic ones (eq 1−3). We follow an iterative procedure that is found to converge well.

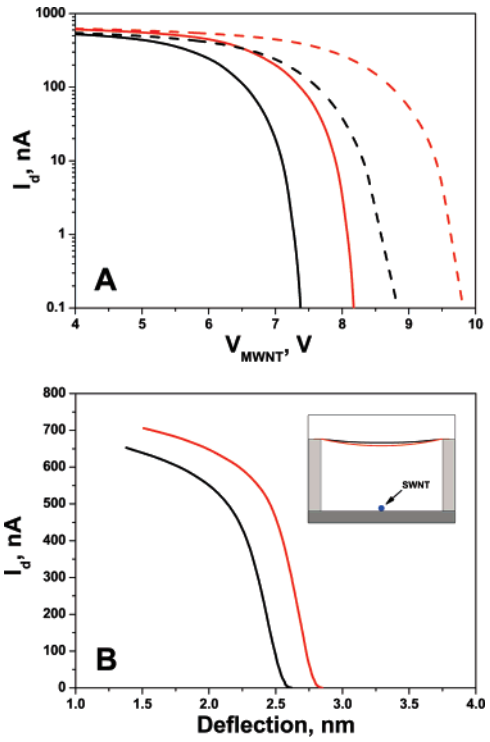

Figure 2. Drain current vs V_{MWNT} (A) and drain current vs maximum deflection of the MWNT (from unbent shape) (B) for design 1. Black line: $V_{BG} = -7$ V; red line: $V_{BG} = -8$ V. Dashed lines: the same dependence for the case when the MWNT is not allowed to bend. The source-drain voltage is 50 mV. Inset in (B) shows the bent MWNT shapes for on-state (black line) and near pinch-off state (red line).

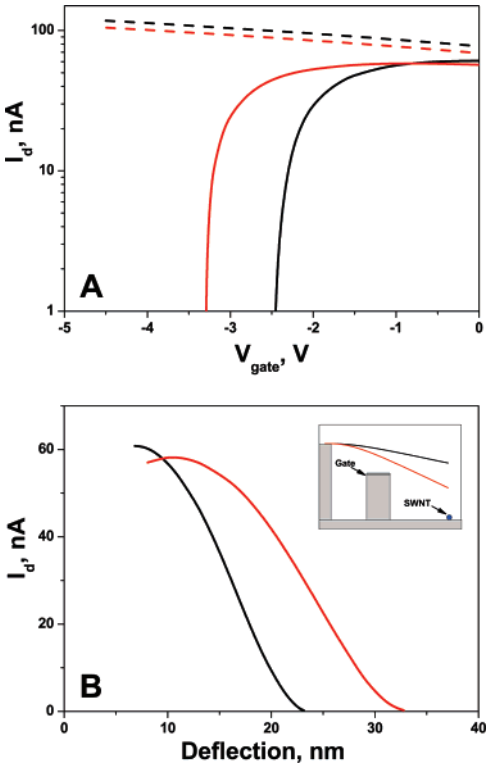

Figure 3. Drain current vs V_{gate} (A) and drain current vs maximum deflection of MWNT (B) for design 2a (black line) and design 2b (red line). The nonmonotonic behavior is due to direct electrostatic coupling between the gate and the SWNT. Dashed lines: the same dependence for the case when the MWNT is not allowed to bend. The source-drain voltage is 50 mV. Inset in (B) shows the bent MWNT shapes for on-state (black line) and near pinch-off state (red line).

For design 1, we choose a long and thin MWNT with high Young's modulus[23] $E = 1200$ GPa and residual tension $T_0 = 0$ (the value of T_0 for a particular device depends on the details of the fabrication).

The drain current dependence on voltage applied to MWNT is shown on Figure 2A for two different back-gate voltages $V_{BG} = -7$ V and $V_{BG} = -8$ V. To illustrate the advantage that the mechanical bending brings, we plot the same dependence for the device with fixed MWNT. Comparison shows that, due to allowed bending, first, the threshold voltage is reduced, and second, the subthreshold slope becomes significantly steeper, reaching 32 mV/decade for $V_{BG} = -8$ V. In Figure 2B, we plot the drain current versus the maximum deflection of the MWNT from unbent shape. Note that a relatively small deflection has a substantial effect.

We have investigated the dependence of the subthreshold slope on the support height H and the diameter of the MWNT gate. For $H \geq 20$ nm, the subthreshold slope increases linearly with H reaching the thermal limit 60 mV/decade for $H \cong 60$ nm. The dependence on the MWNT diameter is very weak.

In design 2, a MWNT cantilever with a large diameter is used to avoid pull-in. The stiffness of CNTs is known to decrease with increasing diameter due to rippling deformations,[23−25] which is why we use a lower Young's modulus for the MWNT gate in design 2. The distribution of the measured Young's moduli is quite wide and depends on tube quality and measurement technique,[26] and the value we use, $E = 400$ GPa, is reasonable for good quality tubes. A lower value of stiffness would result in inferior performance and, eventually, problems with pull-in. We investigate two different support heights. In case of lower support height (design 2a), we find that a lower V_{MWNT} must be applied in order to avoid pull-in, while for higher support (design 2b) higher V_{MWNT} is possible. Higher V_{MWNT} leads to sharper switching characteristics but places higher demands on the stiffness of the suspended tubes.

In Figure 3A, we plot the drain current versus gate voltage for design 2a and design 2b. The effective subthreshold slopes near pinch-off reach 25 and 15 mV/decade, and the threshold gate voltages are −2.5 and −3.3 V, respectively. In Figure 3B, we show the drain current versus the deflection of the MWNT tip for designs 2a and 2b. The cantilever design, not limited by nonlinear tension, allows for wider range of displacements than the design with doubly clamped MWNT, which results in steeper switching, but the limitation on the applicable voltage due to rise of pull-in limits the on-state current.

In conclusion, we have developed a model that describes the static operation of a CNTFET with a suspended MWNT gate. We have presented two designs based on doubly and singly clamped MWNT gates. For the former, we have provided direct comparison to the fixed-gate CNTFET. We

have shown that the proposed devices exhibit sharp switching, characterized by superexponential dependence of drain current on gate voltage, with an effective subthreshold slope down to 15 mV/decade.

We have also shown that the deflection of the MWNT can be sensed by monitoring the drain current. As we can see from Figures 2B and 3B, in a range of deflections, the dependence of current on deflection is linear, and at higher deflections, the current drops exponentially with increasing deflection. This provides an alternative detection scheme to the RF mixing experiments[7,8] and allows a direct measurement of the instantaneous deflection of a single suspended nanotube. It also suggests an alternative to the displacement sensing scheme relying on strain-induced conductance changes, which has been recently proposed by Stampfer et al.[27]

Acknowledgment. We acknowledge the support of the European Commission (EC) through the FP6 research project NanoRF (contract number FP6-2005-028158). This publication reflects the views of the authors and not necessarily those of the EC. The EC is not liable for any use that may be made of the information contained herein. J.K. also acknowledges financial support by the Swedish Foundation for Strategic Research. We are grateful to Andreas Isacsson, Klas Engström, Johannes Svensson, Robert Rehammar, and Eleanor Campbell for valuable discussions. We also thank Robert Rehammar for the help with device pictures.

References

(1) Rueckes, T.; Kim, K.; Joselevich, E.; Tseng, G. Y.; Cheung, C.-L.; Lieber, C. M. *Science* **2000**, *289*, 94.
(2) Maslov, L. *Nanotechnology* **2006**, *17*, 2475.
(3) Kinaret, J. M.; Nord, T.; Viefers, S. *Appl. Phys. Lett.* **2003**, *82*, 1287.
(4) Jonsson, L. M.; Nord, T.; Viefers, S.; Kinaret, J. M. *J. Appl. Phys.* **2004**, *96*, 629.
(5) Hwang, H. J.; Kang, J. W. *Physica E* **2005**, *27*, 163.
(6) Jonsson, L. M.; Axelsson, S.; Nord, T.; Viefers, S.; Kinaret, J. M. *Nanotechnology* **2004**, *15*, 1497.
(7) Sazonova, V.; Yaish, Y.; Ustunel, H.; Roundy, D.; Arias, T. A.; McEuen, P. L. *Nature* **2004**, *431*, 284.
(8) Witkamp, B.; Poot, M.; van der Zant, H. S. J. *Nano Lett.* **2006**, *6*, 2904.
(9) Lee, S.-W.; Lee, D.-S.; Morjan, R. E; Jhang, S. H.; Sveningsson, M.; Nerushev, O. A.; Park, Y. W.; Campbell, E. B. *Nano Lett.* **2004**, *4*, 2027.
(10) Bachtold, A.; Hadley, P.; Nakanishi, T.; Dekker, C. *Science* **2001**, *294*, 1317.
(11) Chen, Z.; Appenzeller, J.; Lin, Y.-M.; Sippel-Oakley, J.; Rinzler, A. G.; Tang, J.; Wind, S. J.; Solomon, P. M.; Avouris, P. *Science* **2006**, *311*, 5768.
(12) Wind, S. J.; Appenzeller, J.; Martel, R.; Derycke, V.; Avouris, P. *Appl. Phys. Lett.* **2002**, *80*, 3817.
(13) Abelé, N.; Fritschi, R.; Boukart, K.; Casset, F.; Ancey, P.; Ionescu, A. *IEDM Tech. Dig.* **2005**, 1075.
(14) Engström, K. E.; Kinaret, J. M. *IEEE Electron Device Lett.* **2006**, *27*, 988.
(15) Lee, D.-S.; Svensson, J.; Lee, S. W.; Park, Y. W.; Campbell, E. B. *J. Nanosci. Nanotechnol.* **2006**, *6*, 1325.
(16) Guo, J.; Alam, M. A. *Appl. Phys. Lett.* **2005**, *86*, 023105.
(17) Tersoff, J.; Freitag, M.; Tsang, J. C.; Avouris, Ph. *Appl. Phys. Lett.* **2005**, *86*, 263108.
(18) Perebeinos, V.; Tersoff, J.; Avouris, Ph. *Nano Lett.* **2006**, *6*, 205.
(19) Zhou, X.; Park, J. Y.; Huang, S.; Liu, J.; McEuen, P. *Phys. Rev. Lett.* **2005**, *95*, 146805.
(20) Paris, F.; Canas, J. *Boundary Element Method: Fundamentals and Applications*; Oxford University Press: New York, 1997.
(21) Shi, F.; Ramesh, P.; Mukherjee, S. *Comput. Struct.* **1995**, *56*, 769.
(22) Dresselhaus, M. S.; Dresselhaus, G.; Avouris, Ph. *Carbon Nanotubes: Synthesis, Structure, Properties and Application*; Springer-Verlag: Heidelberg, 2001; Vol. 80.
(23) Poncharal, P.; Wang, Z. L.; Ugarte, D.; de Heer, W. A. *Science* **1999**, *283*, 1513.
(24) Wang, X. Y.; Wang, X. *Composites Part B* **2004**, *35*, 79.
(25) Lefèvre, R.; Goffman, M. F.; Derycke, V.; Miko, C.; Forró, L.; Bourgoin, J. P.; Hesto, P. *Phys. Rev. Lett* **2005**, *95*, 185504.
(26) Demczyk, B. G.; Wang, Y. M.; Cumings, J.; Hetman, M.; Han, W.; Zettl, A.; Ritchie, R. O. *Mater. Sci. Eng., A* **2002**, *334*, 173.
(27) Stampfer, C.; Jungen, A.; Linderman, R.; Obergfell, D.; Roth, S.; Hierold, C. *Nano Lett.* **2006**, *6*, 1449.

NL070891+